Design of Unequal Error Protection for MIMO-OFDM Systems with Hierarchical Signal Constellations

Yujin Noh, Heunchul Lee, Wonjun Lee, and Inkyu Lee

Abstract: **In multimedia communication systems, efficient transmission system design should incorporate the use of matching unequal error protection (UEP), since source coders exhibit unequal bit error sensitivity. In this paper, we present UEP schemes which exploit differences in bit error protection levels in orthogonal frequency division multiplexing (OFDM) systems over frequency selective fading channels. We introduce an UEP scheme which improves the link performance with multiple transmit and receive antennas. Especially, we propose a new receiver structure based on two stage Maximum Likelihood detection (MLD) schemes which can approach the performance of a full search MLD receiver with much reduced computational complexity. In the performance analysis, we derive a generalized pairwise error probability expression for the proposed UEP schemes. Simulation results show that the proposed schemes achieve a significant performance gain over the conventional equal error protection (EEP) scheme.**

Index Terms: **Multiple-input multiple-output orthogonl frequency division multiplexing (MIMO-OFDM), multistage decoding (MSD), performance evaluation, unequal error protection (UEP).**

I. INTRODUCTION

Next generation wireless communication systems are expected to provide reliable transmission over fading channels. Bit streams from most real world source coding algorithms for speech, audio, images and video exhibit unequal bit error sensitivity for different bits. In the conventional system, error protection needs to be designed for the most sensitive bits, because those bits will dominate the overall detection performance. In such equal error protection (EEP) systems, this results in the waste of resource for the protection of the least sensitive bits, since they are assigned the same protection level as the most sensitive bits.

In contrast, the unequal error protection (UEP) [1], [2] receiver matches the protection level according to the system requirement, and thus can save system resources. When all the bits in the bit stream do not require the same error protection, we can improve the overall efficiency by applying UEP at no extra bandwidth or power requirement. The UEP schemes divide the source data into two or more groups and assign different protection levels to each group. The most important bits, defined as base information (BI), are protected with more redundancy, while the least important bits, defined as refinement information (RI), are restored with less protection. For example, it has been determined in [3] that, for good voice quality, the most sensitive bits of a G.723.1 frame cannot tolerate a bit error rate (BER) higher than 5×10^{-5}, while the remaining bits can tolerate a BER as high as 10^{-3}.

Several UEP schemes have been employed in many digital communication systems to jointly optimize the transmission schemes with the digital source. A UEP scheme based on rate compatible punctured convolutional (RCPC) codes [4] has been studied in [5]. The design of an error correction scheme is usually carried out by selecting a fixed channel code with the same error correction capability for all the data to be transmitted, where the fixed code is designed to handle the worst case of average channel/source conditions and the most error sensitive source bits. To make the best use of the limited resources, it is necessary to match the error protection level provided by the channel code to the error sensitivity. The RCPC codes meet such requirements of providing a flexible UEP [5]. Punctured bits in the RCPC codes represent savings in bit rate (or bandwidth) without loss of quality. Alternatively, the gain of UEP over EEP can be converted into a power gain. Other previous approaches include nonstandard signal set signal partitioning and multistage decoding (MSD) [1], [6], [7] techniques which provide good UEP capabilities. The coding scheme is designed in such a way that the most important information bits result in a better error rate than other information bits. A hierarchical signal constellation of an nonuniform signal constellation is also a natural strategy to provide the UEP capability [8].

Multiple-input multiple-output (MIMO) [9], [10] systems have attracted much attention to provide high-speed data for next generation communication systems with multiple antennas at the transmitter and receiver side. As the demand for higher bit rates increases, it becomes important to use the spectral source more efficiently. For wideband systems, both single carrier and multi-carrier systems can be applied to combat frequency selective channels. Equalization is one choice for the single carrier approach [11], whereas orthogonal frequency division multiplexing (OFDM) utilizes multiple subcarriers to cope with frequency selectivity caused by multipath fadings for the multicarrier approach [12]–[15]. For example, the wireless local area network (WLAN) system defined by the IEEE 802.11a standard adopts the OFDM in packet-based communications operating in the unlicensed 5 GHz band. In this paper, we propose a UEP scheme for MIMO-OFDM which combines OFDM with MIMO systems. The proposed UEP schemes employ a hierar-

Manuscript received December 28, 2006.

Y. Noh was with School of Electrical Eng., Korea University, Seoul, Korea. She is now with LG Electronics, Anyang, Korea, email: gajadoll@lge.com.

H. Lee and I. Lee are with School of Electrical Eng., Korea University, Seoul, Korea, email: heunchul@wireless.korea.ac.kr, inkyu@korea.ac.kr.

W. Lee is with Dept. of Computer Science and Engineering, Korea University, Seoul, Korea. email: wlee@korea.ac.kr.

This work was supported in part by the Ministry of Information and Communication (MIC), Korea, under the Information Technology Research Center (ITRC) support program, supervised by the Institute of Information Technology Assessment (IITA) and in part by grant No. R01-2006-000-11112-0 from the Basic Research Program of the Korea Science & Engineering Foundation.

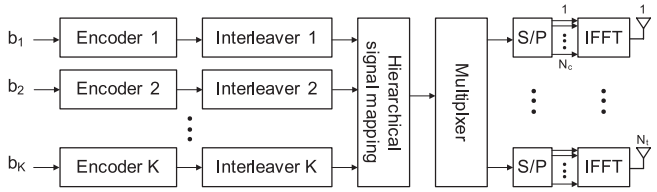

Fig. 1. Transmitter structure for the UEP

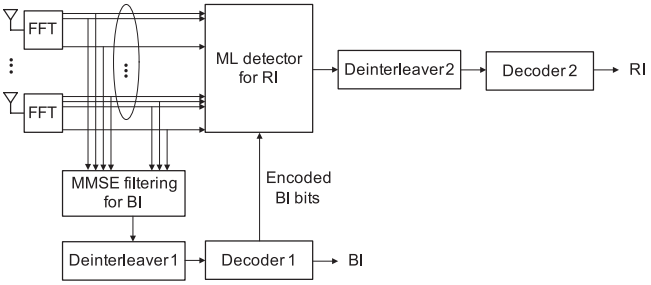

Fig. 2. Receiver structure for the proposed UEP

chical signal mapping based on both minimum mean square error (MMSE) and maximum likelihood (ML) detectors. We show that a significant performance gain for BI is achieved compared with an EEP scheme. We investigate the performance of the proposed UEP in the nonuniform signal constellation.

While the maximum likelihood detection (MLD) exhibits the optimum performance, it is often too complicated to be applied in practice. Thus, much interest has been focused on reducing the complexity of the original MLD method [16]–[20]. In this paper, we propose an efficient MLD receiver operating in two stages. The proposed detector estimates the BI bits using an MMSE detector first, then the remaining RI bits are processed by MLD. Simulation results show that the proposed two stage MLD scheme can achieve a near ML performance with reduced complexity.

Also we derive the generalized pairwise error probability (PEP) for the proposed UEP scheme in MIMO-OFDM systems. Based on the PEP analysis, we can optimize the hierarchial nonuniform constellation to maximize the coding gain.

The organization of the paper is as follows: In Section II, we present the system overview. In Section III, we propose a new UEP scheme and a two stage MLD receiver. Then, we evaluate the PEP bound of the proposed UEP scheme in Section IV. Section V shows the simulation results for MIMO-OFDM. Finally, the paper is terminated with discussions in Section VI.

II. SYSTEM OVERVIEW

In this section, we consider an OFDM system with N_t transmit and N_r receive antennas. Fig. 1 shows the transmitter configuration of the UEP system, where N_c indicates the number of subcarriers. Here, K different bit sensitivity groups are transmitted through parallel transmission substreams with independent encoders and bit-interleavers. A key function block in this structure is a hierarchical signal mapping [21]. The hierarchical signal mapping offers different levels of protection to the transmitted bits in a message symbol according to their priorities. Thus, information bits are distributed to different bit-sensitivity groups.

For the channel model, we make the following assumptions. Considering the time domain channel impulse response between the ith transmit and the jth receiver antenna, the frequency selective channel can be modeled as

$$h^{i,j}(\tau) = \sum_{n=1}^{L} \bar{h}^{i,j}(n)\delta(\tau - \tau_n)$$

where the channel coefficients $\bar{h}^{i,j}(n)$ are independent complex Gaussian with zero mean, $\delta(\cdot)$ and τ_n stand for the Dirac delta function and the nth time propagation delay, respectively, and L denotes the number of channel taps. It follows that the channel frequency response between the ith transmit and the jth receive antenna can be expressed by

$$H_k^{i,j} = \sum_{n=1}^{L} \bar{h}^{i,j}(n)e^{-j2\pi k\tau_n/N_cT_s} = \bar{\mathbf{h}}_{i,j}^{*}\mathbf{w}_k \qquad (1)$$

where T_s represents the sampling period and $\bar{\mathbf{h}}_{i,j}^{*}$ and $\mathbf{w}_k$ are defined as $\bar{\mathbf{h}}_{i,j} = [\bar{h}^{i,j}(1)\ \bar{h}^{i,j}(2)\ \cdots\ \bar{h}^{i,j}(L)]^*$ and $\mathbf{w}_k = [e^{-j2\pi k\tau_1/N_cT_s}\ e^{-j2\pi k\tau_2/N_cT_s}\ \cdots\ e^{-j2\pi k\tau_L/N_cT_s}]^T$, respectively. Here, $(\cdot)^T$ and $(\cdot)^*$ indicate the transpose and the complex-conjugate transpose, respectively. Note that $|H_k^{i,j}|$ is Rayleigh distributed.

Let us define the N_t-dimensional complex transmitted signal vector $\mathbf{x}_k$ and the N_r-dimensional complex received signal vector $\mathbf{y}_k$. Then, the received signal at the kth subcarrier can be written as

$$\mathbf{y}_k = \sqrt{E_s}\mathbf{H}_k\mathbf{x}_k + \mathbf{n}_k$$

where E_s is the symbol energy and

$$\mathbf{H}_k = \begin{bmatrix} H_k^{1,1} & \cdots & H_k^{N_t,1} \\ \vdots & \ddots & \vdots \\ H_k^{1,N_r} & \cdots & H_k^{N_t,N_r} \end{bmatrix}, \mathbf{n}_k = \begin{bmatrix} n_k^1 \\ \vdots \\ n_{N_r}^k \end{bmatrix}.$$

Here, we assume that the transmitted signal power is normalized to unity and distributed equally over N_t transmit antennas. Thus, the covariance matrix of $\mathbf{x}_k$ equals $E[\mathbf{x}_k\mathbf{x}_k^*] = \mathbf{I}_{N_t}$ where $E[\cdot]$ and $\mathbf{I}_{N_t}$ indicate expectation and an identity matrix of size N_t, respectively. The additive noise terms in $\mathbf{n}_k$ are assumed to be independent and identically-distributed (i.i.d.) complex zero mean Gaussian with variance σ_n^2.

III. PROPOSED UEP STRUCTURE

In this section, we first propose a UEP scheme with the hierarchical signal mapping. Then, the two stage MLD scheme is also presented.

A. Hierarchical Signal Mapping

Fig. 2 exhibits the receiver structure for the proposed UEP. The receiver is assumed to have perfect knowledge of the channel state information. After the FFT demodulation, the received

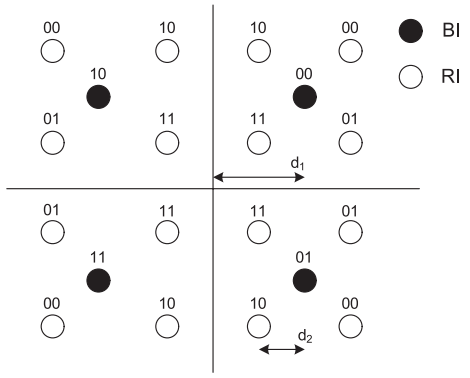

Fig. 3. Hierarchical signal mapping for 16QAM

signals can be processed either by MMSE filtering or MLD. The ML detection achieves the optimum performance at the expense of increased complexity compared to the MMSE filtering. After demultiplexing, each parallel substream is independently bit-deinterleaved and decoded.

As an example, for the 16QAM case, we can consider two incoming data streams ($K = 2$) where b_1 and b_2 denote the BI and the RI bits, respectively. In the BI stream, two bits out of four are assigned to the most important bit positions, while in the RI stream the remaining two bits are assigned to the least important bit positions. In Fig. 3, the hierarchical signal constellation for 16QAM is presented [21], [22]. The hierarchical signal constellation is designed such that the BI bits are selected as one of four fictitious symbols (black circles), whereas the RI bits are treated as one of four symbols (empty circles) surrounding the selected fictitious symbol. In other words, the constellation consists of "clouds" of subconstellations which account for the RI, while the BI is represented by the position of the clouds. Thus, incorrect detection of the BI gives rise to subsequent decision errors for the RI. In Fig. 3, $2d_1$ represents the distance between the two fictitious symbols, whereas $2d_2$ corresponds to the distance between two neighboring symbols within a subconstellation. By controlling the distance between d_1 and d_2 with a parameter $\lambda = \frac{d_2}{d_1}$ in the nonuniform signal constellation, we can change relative protection levels for two bit streams. When $0 < \lambda < \frac{1}{2}$, the BI bits are given a higher priority while the RI bits are applied with better protection for $\frac{1}{2} < \lambda < 1$, compared to the conventional 16QAM. If λ gets smaller, the performance of the BI improves at the expense of that of the RI. For $\lambda = 0$, the signal constellation becomes a uniform 4QAM with no RI. Also, for $\lambda = \frac{1}{2}$, the signal constellation becomes a uniform 16QAM where both BI and RI exhibit the same priority.

B. Proposed Two Stage MLD Scheme

As will be shown in the simulation section, it turns out that the BI performance of the proposed UEP based on MMSE filtering is better than the performance of EEP based on MLD. This motivates us to consider the receiver structure which consists of the two stage MLD as shown in Fig. 4. In the first stage, we process the BI based on the MMSE filtering with low complexity.

Now we will illustrate a receiver based on MMSE filtering. To simplify the notation, we omit the subscript k for the rest of

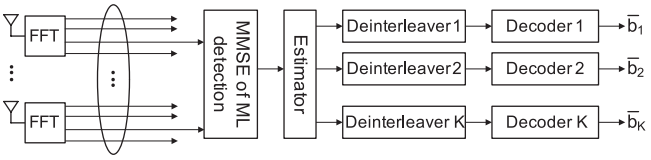

Fig. 4. Receiver structure for the two stage MLD

this section. Using the MMSE criterion, the equalizer matrix $\mathbf{G}$ is formulated to minimize the mean square values of the error $\mathbf{e} = \mathbf{x} - \mathbf{G}\mathbf{y}$. Then, the equalization matrix $\mathbf{G}$ can be obtained by invoking the orthogonality principle. Thus, it follows

$$E[\mathbf{e}\mathbf{y}^*] = \mathbf{E}[(\mathbf{x} - \mathbf{G}\mathbf{y})\,\mathbf{y}^*] = \mathbf{0}.$$

First denoting $\alpha = \frac{\sigma_n^2}{E_s}$, we obtain the equalizer matrix $\mathbf{G}$ as

$$\mathbf{G} = \left(\mathbf{H}^\dagger\mathbf{H} + \alpha\mathbf{I}_{N_t}\right)^{-1}\mathbf{H}.$$

Let the equalizer output be $\mathbf{z} = \mathbf{G}\mathbf{y}$. Defining $\mathbf{g_t}$ as the tth row of $\mathbf{G}$, the tth element of the equalizer output is given as

$$\begin{aligned} z_t &= \mathbf{g}_t\mathbf{H}\mathbf{x} + \mathbf{g}_t\mathbf{n} \\ &= \mathbf{g}_t\mathbf{h}_t x_t + \sum_{i=1, i\neq t}^{N_t} \mathbf{g}_t\mathbf{h}_i x_i + \mathbf{g}_t\mathbf{n} \\ &= \beta x_t + \omega \end{aligned}$$

where β and ω are defined as $\mathbf{g}_t\mathbf{h}_t$ and $\sum_{i=1,i\neq t}^{N_t}\mathbf{g}_t\mathbf{h}_i x_i + \mathbf{g}_t\mathbf{n}$, respectively. Since those terms in ω are assumed to be independent of each other, the variance of ω is computed as

$$\sigma_w^2 = \sum_{i=1, i\neq t}^{N_t} \|\mathbf{g}_t\mathbf{h}_i\|^2 E_s + \|\mathbf{g}_t\|^2\sigma_n^2.$$

After the biased term is properly scaled, the input of the unbiased demapper can be written as

$$\hat{x}_t = z_t/\beta = x_t + v$$

where v is the complex noise with variance $\sigma_v^2 = \sigma_w^2/\|\beta\|^2$.

In what follows, we briefly describe the Log-Likelihood Ratio (LLR) computation [23] for soft bit information of BI bits. Let $\mathcal{S}_{BI}^t$ be a set of constellation symbols and denote x_{BI}^t as its element. We represent the ith bit of x_{BI}^t by $b_{BI}^{t,i}$ and define two mutually exclusive subsets of $\mathcal{S}_{BI}^t$ as $\mathcal{S}_{BI}^{t,0} = \{x_{BI}^t | b_{BI}^{t,i} = 0\}$ and $\mathcal{S}_{BI}^{t,1} = \{x_{BI}^t | b_{BI}^{t,i} = 1\}$ for $i = 1, 2, \cdots, m_b$ where m_b is the number of BI bits. Note that $|\mathcal{S}_{BI}^t|$ is equal to the constellation size M. Then, the LLR of $b_{BI}^{t,i}$ [23] can be represented by

$$LLR(b_{BI}^{t,i}) = \log \frac{\sum_{x_{BI}^t \in \mathcal{S}_{BI}^{t,0}} \exp\left(-\frac{|\hat{x}_t - x_{BI}^t|^2}{\sigma_v^2}\right)}{\sum_{x_{BI}^t \in \mathcal{S}_{BI}^{t,1}} \exp\left(-\frac{|\hat{x}_t - x_{BI}^t|^2}{\sigma_v^2}\right)}. \quad (2)$$

Here, we assume that v makes complex Gaussian distribution for analytic conveniences.

When the BI bits are estimated using the MMSE filtering, the detection performance becomes poor even if the RI bits are

detected using ML. This indicates that the overall performance is mostly determined by the accuracy of the BI bit estimation. Thus, in order to improve the BI detection performance, we employ a decision feedback method [24] by using decoder outputs to enhance the accuracy of the BI estimates at the first stage. After the BI decisions obtained from the MMSE filtering are passed to the decoder, the decoded outputs are re-encoded. Note that the encoded bits can be obtained directly from the decoding trellis without any extra processing. Then, in the second stage, the MLD detects the RI bits in a smaller coset by utilizing the re-encoded BI bits.

Let us define $b_{RI}^{t,i}$ $(i = 1, 2, \cdots, m_r)$ for RI similarly as in $b_{BI}^{t,i}$, where m_r represents the number of RI bits. Denote $\mathbf{S}_{RI}^{t,d}, d = 1$ or 0, as a set of all symbol vectors with $b_{RI}^{t,i} = d$. Here, the BI bits in a symbol vector $\mathbf{x} \in \mathbf{S}_{RI}^{t,d}$ are fixed with the decisions made from the first stage to reduce the search size. The number of elements in such a set is $2^{N_t m_r - 1}$. Then, the LLR for RI is given as

$$LLR(b_{RI}^{t,i}) = \log \frac{\sum_{\mathbf{x} \in \mathbf{S}_{RI}^{t,0}} \exp\left(- \frac{\|\mathbf{y} - \sqrt{E_s}\mathbf{H}\mathbf{x}\|^2}{\sigma_n^2} \right)}{\sum_{\mathbf{x} \in \mathbf{S}_{RI}^{t,1}} \exp\left(- \frac{\|\mathbf{y} - \sqrt{E_s}\mathbf{H}\mathbf{x}\|^2}{\sigma_n^2} \right)}.$$

We summarize the proposed two stage MLD procedure as follows:

- In the first stage, the LLR values for the BI bits are computed using (2) based on the MMSE filtering.
- The computed LLR values for BI are passed to the decoder.
- The encoded BI bits transfer to the second stage for the MLD.
- In the second stage, by fixing the BI bits in the hierarchical signal mapping, the LLR values for the RI bits are computed with MLD.
- Finally, these LLR values are passed to the decoder for the RI bits.

For example, for the 16QAM case with $m_b = m_r = 2$, if the encoded BI bits correspond to 00, then we perform a local MLD for four symbols surrounding 00 in Fig. 3 to obtain the LLR values for RI. It should be pointed out that the computational complexity of the two stage MLD is mainly determined by the number of RI bits. Therefore, compared to the full ML detector, the proposed two stage MLD scheme can reduce the number of candidate search from $2^{N_t \cdot (m_b + m_r)}$ to $2^{N_t \cdot m_r}$.

IV. GENERALIZED PAIRWISE ERROR PROBABILITY EVALUATION

In this section, we will evaluate the generalized pairwise error probability (PEP) of the proposed UEP scheme for MIMO-OFDM systems with nonuniform constellation for frequency selective block fading channels. Assuming that $\mathbf{x}$ is transmitted, we have the average PEP [25] that ML chooses $\hat{\mathbf{x}}$ over $\mathbf{x}$ as

$$P\left(\mathbf{x} \to \hat{\mathbf{x}} | \{\mathbf{H}_k\}_{k=1}^{N_c}\right) = P\left(\sum_{k=1}^{N_c} \left(\|\mathbf{y}_k - \sqrt{E_s}\mathbf{H}_k\mathbf{x}_k\|^2 - \|\mathbf{y}_k - \sqrt{E_s}\mathbf{H}_k\hat{\mathbf{x}}_k\|^2 \right) > 0 | \{\mathbf{H}_k\}_{k=1}^{N_c} \right).$$

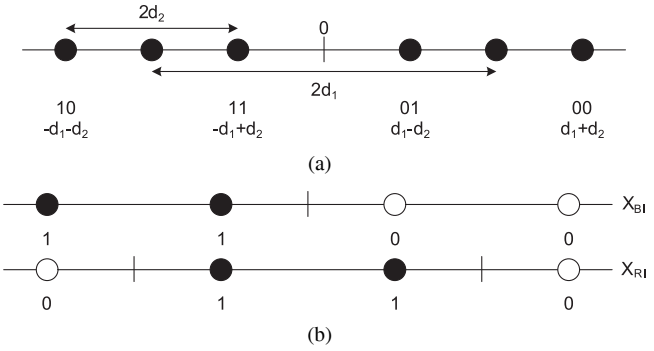

Fig. 5. 4-PAM nonuniform constellation for the UEP

From now on, we will analyze the above PEP for BI and RI separately. In square constellations such as 16QAM, there exist symmetries between inphase and quadrature components. Therefore, in order to simplify the analysis, we consider one dimensional 4PAM nonuniform constellation [26] for either inphase or quadrature component of 16QAM. We denote $\mathbf{x}_{\mathrm{BI}}$ and $\mathbf{x}_{\mathrm{RI}}$ as the BI and the RI bits of transmitted sequence $\mathbf{x}$, respectively.

Fig. 5 illustrates the 4PAM nonuniform constellation. As shown in Fig. 5(a), the 4PAM symbols are located at $-d_1 - d_2$, $-d_1 + d_2$, $d_1 - d_2$, and $d_1 + d_2$. In this constellation, the first bit in the symbol label represents $\mathbf{x}^{\mathrm{BI}}$, whereas the second bit denotes $\mathbf{x}^{\mathrm{RI}}$. In Fig. 5(b), the decision boundaries for $\mathbf{x}^{\mathrm{BI}}$ and $\mathbf{x}^{\mathrm{RI}}$ are shown. The average probability of error for nonuniform constellations in single-input single-output (SISO) systems is presented in [27]. To understand the nonuniform constellation property in Fig. 5, we first analyze the error probability for BI. For $\mathbf{x}^{\mathrm{BI}}$, the probability of error when symbol 10 is transmitted is given by $Q\left(\frac{d_1+d_2}{\sigma_n}\right)$. Similarly, the error probability when symbol 11 is transmitted is obtained by $Q\left(\frac{d_1-d_2}{\sigma_n}\right)$. Thus, the average bit error probability for BI is given by

$$\frac{1}{2}Q\left(\frac{d_1 + d_2}{\sigma_n}\right) + \frac{1}{2}Q\left(\frac{d_1 - d_2}{\sigma_n}\right).$$

As for the performance of RI, the bit error probabilities when symbols 10 and 11 are transmitted are given by $Q\left(\frac{d_2}{\sigma_n}\right) - Q\left(\frac{2d_1+d_2}{\sigma_n}\right)$ and $Q\left(\frac{d_2}{\sigma_n}\right) + Q\left(\frac{2d_1-d_2}{\sigma_n}\right)$, respectively. Thus, the average bit error probability for RI is given by

$$Q\left(\frac{d_2}{\sigma_n}\right) - \frac{1}{2}Q\left(\frac{2d_1 + d_2}{\sigma_n}\right) + \frac{1}{2}Q\left(\frac{2d_1 - d_2}{\sigma_n}\right).$$

Now, for the proposed MIMO systems, we consider the average PEP for BI that the ML choose $\hat{\mathbf{x}}^{\mathrm{BI}}$ over $\mathbf{x}^{\mathrm{BI}}$ as

$$P\left(\mathbf{x}^{\mathrm{BI}} \to \hat{\mathbf{x}}^{\mathrm{BI}} | \{\mathbf{H}_k\}_{k=1}^{N_c}\right) \le \exp\left(-\frac{E_b}{4N_0} \sum_{k=1}^{N_c} \|\mathbf{H}_k \mathbf{e}_k^{\mathrm{BI}}\|^2 \right) \tag{3}$$

where E_b is the bit energy and $\mathbf{e}_k^{\mathrm{BI}} = \hat{\mathbf{x}}_k^{\mathrm{BI}} - \mathbf{x}_k^{\mathrm{BI}}$.

In analyzing the above bound, we will take into account only the most-likely error events where $\mathbf{e}_k^{\mathrm{BI}}$ contains at most one nonzero element at any k, because the contribution from error events with more than two nonzero elements can be neglected for high SNR [28]. Thus, we consider the most-likely error events with one nonzero value at the Δth element, noting that the actual value of Δ $(1 \le \Delta \le N_t)$ does not affect the PEP analysis. Then, there are three possible error events $\mathbf{e}_k^{\mathrm{BI}}$: $2(d_1+d_2)\mathbf{1}_{\mathbf{\Delta}}$, $2(d_1-d_2)\mathbf{1}_{\mathbf{\Delta}}$, and $2d_1\mathbf{1}_{\mathbf{\Delta}}$ where $\mathbf{1}_{\mathbf{\Delta}}$ denotes a $N_t \times 1$ unit vector with one at the Δth position.

Now, we consider the term $\sum_{k=1}^{N_c}\left\|\mathbf{H}_k\mathbf{e}_k^{\mathrm{BI}}\right\|^2$ in (3). In order to compute this term, we denote the jth row of $\mathbf{H}_k$ as $\mathbf{h}_{j,k}^*$. Then, from (1), $\mathbf{h}_{j,k}^*$ can be expressed as

$$\mathbf{h}_{j,k}^* = \left[\bar{\mathbf{h}}_{1,j}^*\ \bar{\mathbf{h}}_{2,j}^*\cdots\bar{\mathbf{h}}_{N_t,j}^*\right](\mathbf{w}_k\otimes\mathbf{I}_{N_t}) = \tilde{\mathbf{h}}_j^*\mathbf{W}_k$$

where $\tilde{\mathbf{h}}_j^* = \left[\bar{\mathbf{h}}_{1,j}^*\ \bar{\mathbf{h}}_{2,j}^*\cdots\bar{\mathbf{h}}_{N_t,j}^*\right]$ is a row vector of length LN_t and $\otimes$ represents the Kronecker product. Note that the elements of $\tilde{\mathbf{h}}_j$ are uncorrelated with each other.

Denoting $\mathbf{e}_k^{\mathrm{BI}}$ as $c_k\mathbf{1}_{\mathbf{\Delta}}$ where $c_k = 0, 2\,(d_1 \pm d_2)$ or $2d_1$, we can express $\sum_{k=1}^{N_c}\left\|\mathbf{H}_k\mathbf{e}_k^{BI}\right\|^2$ as

$$\begin{aligned}\sum_{k=1}^{N_c}\left\|\mathbf{H}_k\mathbf{e}_k^{BI}\right\|^2 &= \sum_{k=1}^{N_c}\sum_{j=1}^{N_r}\left|\mathbf{h}_{j,k}^*\mathbf{e}_k^{BI}\right|^2 = \sum_{k=1}^{N_c}c_k^2\sum_{j=1}^{N_r}\left|\tilde{\mathbf{h}}_j^*\tilde{\mathbf{e}}_k^{BI}\right|^2\\ &= \sum_{k=1}^{N_c}c_k^2\sum_{j=1}^{N_r}\tilde{\mathbf{h}}_j^*\tilde{\mathbf{E}}_k^{BI}\tilde{\mathbf{h}}_j \qquad (4)\end{aligned}$$

where $\tilde{\mathbf{e}}_k^{BI} = \mathbf{W}_k\mathbf{1}_\Delta$ and $\tilde{\mathbf{E}}_k^{BI} = \tilde{\mathbf{e}}_k^{BI}\cdot\left(\tilde{\mathbf{e}}_k^{BI}\right)^*$.

As c_k can have three different nonzero values, we define $\mathbf{S}_{\mathbf{1}}^{\mathrm{BI}}$, $\mathbf{S}_{\mathbf{2}}^{\mathrm{BI}}$, and $\mathbf{S}_{\mathbf{3}}^{\mathrm{BI}}$ as groups of k at which c_k equals $2(d_1+d_2)$, $2(d_1-d_2)$, and $2d_1$, respectively. Then, we arrange the above terms as

$$\begin{aligned}&\sum_{k=1}^{N_c}\left\|\mathbf{H}_k\mathbf{e}_k^{BI}\right\|^2\\ &= \sum_{k\in\mathbf{S}_{\mathbf{1}}^{\mathrm{BI}}}c_k^2\sum_{j=1}^{N_r}\tilde{\mathbf{h}}_j^*\tilde{\mathbf{E}}_k^{BI}\tilde{\mathbf{h}}_j + \sum_{k\in\mathbf{S}_{\mathbf{2}}^{\mathrm{BI}}}c_k^2\sum_{j=1}^{N_r}\tilde{\mathbf{h}}_j^*\tilde{\mathbf{E}}_k^{BI}\tilde{\mathbf{h}}_j\\ &\quad + \sum_{k\in\mathbf{S}_{\mathbf{3}}^{\mathrm{BI}}}c_k^2\sum_{j=1}^{N_r}\tilde{\mathbf{h}}_j^*\tilde{\mathbf{E}}_k^{BI}\tilde{\mathbf{h}}_j\\ &= 4(d_1+d_2)^2\sum_{j=1}^{N_r}\tilde{\mathbf{h}}_j^*\tilde{\mathbf{E}}_1^{BI}\tilde{\mathbf{h}}_j + 4(d_1-d_2)^2\sum_{j=1}^{N_r}\tilde{\mathbf{h}}_j^*\tilde{\mathbf{E}}_2^{BI}\tilde{\mathbf{h}}_j\\ &\quad + 4d_1^2\sum_{j=1}^{N_r}\tilde{\mathbf{h}}_j^*\tilde{\mathbf{E}}_3^{BI}\tilde{\mathbf{h}}_j.\end{aligned}$$

Since $\tilde{\mathbf{E}}_l^{BI}$ $(l=1,2,3)$ are nonnegative definite Hermitian matrices, we have eigen decomposition as $\tilde{\mathbf{E}}_l^{BI} = \mathbf{P}_l^*\mathbf{\Lambda}_l^{\mathrm{BI}}\mathbf{P}_l$where $\mathbf{P}_l$ and $\mathbf{\Lambda}_l^{\mathrm{BI}}$ denote unitary matrices and real diagonal matrices, respectively. Substituting this into (4), we now get

$$\begin{aligned}\sum_{k=1}^{N_c}\left\|\mathbf{H}_k\mathbf{e}_k^{BI}\right\|^2 &= 4(d_1+d_2)^2\sum_{j=1}^{N_r}\hat{\mathbf{h}}_{j,1}^*\mathbf{\Lambda}_1^{\mathrm{BI}}\hat{\mathbf{h}}_{j,1}\\ &\quad + 4(d_1-d_2)^2\sum_{j=1}^{N_r}\hat{\mathbf{h}}_{j,2}^*\mathbf{\Lambda}_2^{\mathrm{BI}}\hat{\mathbf{h}}_{j,2}\\ &\quad + 4d_1^2\sum_{j=1}^{N_r}\hat{\mathbf{h}}_{j,3}^*\mathbf{\Lambda}_3^{\mathrm{BI}}\hat{\mathbf{h}}_{j,3}\end{aligned}$$

where $\hat{\mathbf{h}}_{j,l} = \mathbf{P}_l\tilde{\mathbf{h}}_j$ represents the column vectors of length LN_t.

Defining $\lambda_{i,l}^{\mathrm{BI}}$ as the ith eigenvalue of $\mathbf{\Lambda}_l^{\mathrm{BI}}$, the above term becomes

$$\begin{aligned}\sum_{k=1}^{N_c}\left\|\mathbf{H}_k\mathbf{e}_k^{BI}\right\|^2 &= 4(d_1+d_2)^2\sum_{i=1}^{LN_t}\sum_{j=1}^{N_r}\lambda_{i,1}^{\mathrm{BI}}\left|\hat{H}_{j,1}^i\right|^2\\ &\quad + 4(d_1-d_2)^2\sum_{i=1}^{LN_t}\sum_{j=1}^{N_r}\lambda_{i,2}^{\mathrm{BI}}\left|\hat{H}_{j,2}^i\right|^2\\ &\quad + 4d_1^2\sum_{i=1}^{LN_t}\sum_{j=1}^{N_r}\lambda_{i,3}^{\mathrm{BI}}\left|\hat{H}_{j,3}^i\right|^2 \qquad (5)\end{aligned}$$

where $\hat{H}_{j,l}^i$ denotes the ith element of $\hat{\mathbf{h}}_{j,l}$ $(l=1,2,3)$.

Since $\mathbf{P}_l$ is unitary, $\left|\hat{H}_{j,l}^i\right|$ is also independent and Rayleigh distributed. Therefore, substituting (5) into the bound (3) yields

$$\begin{aligned}&P\left(\mathbf{x}^{BI}\to\hat{\mathbf{x}}^{BI}\middle|\{\mathbf{H}_k\}_{k=1}^{N_c}\right)\\ &\le\exp\left(-\frac{E_b}{N_o}(d_1+d_2)^2\sum_{i=1}^{LN_t}\sum_{j=1}^{N_r}\lambda_{i,1}^{\mathrm{BI}}\left|\hat{H}_{j,1}^i\right|^2\right)\\ &\quad+\exp\left(-\frac{E_b}{N_o}(d_1-d_2)^2\sum_{i=1}^{LN_t}\sum_{j=1}^{N_r}\lambda_{i,2}^{\mathrm{BI}}\left|\hat{H}_{j,2}^i\right|^2\right)\\ &\quad+\exp\left(-\frac{E_b}{N_o}d_1^2\sum_{i=1}^{LN_t}\sum_{j=1}^{N_r}\lambda_{i,3}^{\mathrm{BI}}\left|\hat{H}_{j,3}^i\right|^2\right). \qquad (6)\end{aligned}$$

To simplify the analysis, we now assume that $\hat{H}_{j,l}^i$ has equal power for all i, j, and l. Then, by averaging the above bound with respect to independent Rayleigh distribution of $\left|\hat{H}_{j,l}^i\right|$, the probability of error bound for BI is finally obtained as

$$\begin{aligned}P\left(\mathbf{x}^{BI}\to\hat{\mathbf{x}}^{BI}\right) &\le \prod_{i=1}^{LN_t}\prod_{j=1}^{N_r}\frac{1}{1+(d_1+d_2)^2\frac{E_b}{N_o}\lambda_{i,1}^{\mathrm{BI}}}\\ &\quad+\prod_{i=1}^{LN_t}\prod_{j=1}^{N_r}\frac{1}{1+(d_1-d_2)^2\frac{E_b}{N_o}\lambda_{i,2}^{\mathrm{BI}}}\\ &\quad+\prod_{i=1}^{LN_t}\prod_{j=1}^{N_r}\frac{1}{1+d_1^2\frac{E_b}{N_o}\lambda_{i,3}^{\mathrm{BI}}}.\end{aligned}$$

Next, we consider the average PEP for RI that the ML chooses $\hat{\mathbf{x}}^{\mathrm{RI}}$ over $\mathbf{x}^{\mathrm{RI}}$ as

$$P\left(\mathbf{x}^{\mathrm{RI}} \to \hat{\mathbf{x}}^{\mathrm{RI}} | \{\mathbf{H}_k\}_{k=1}^{N_c}\right) \le \exp\left(-\frac{E_b}{4N_0}\sum_{k=1}^{N_c}\|\mathbf{H}_k\mathbf{e}_k^{\mathrm{RI}}\|^2\right)$$

where $\mathbf{e}_k^{\mathrm{RI}} = \hat{\mathbf{x}}_k^{\mathrm{RI}} - \mathbf{x}_k^{\mathrm{RI}}$.

Then, there are two possible error events $\mathbf{e}_k^{\mathrm{RI}}$: $2d_1\mathbf{1}_\Delta$ and $2d_2\mathbf{1}_\Delta$. Denoting $\mathbf{e}_k^{\mathrm{RI}} = c_k\mathbf{1}_\Delta$ where $c_k = 2d_1$ or $2d_2$, we define $\mathbf{S_1^{\mathrm{RI}}}$ and $\mathbf{S_2^{\mathrm{RI}}}$ as groups of k at which c_k equals $2d_1$ and $2d_2$, respectively. Then, $\tilde{\mathbf{E}}_l^{\mathrm{RI}}$ $(l = 1, 2)$ is defined similarly as in $\tilde{\mathbf{E}}_l^{\mathrm{BI}}$. Denoting $\lambda_{i,l}^{\mathrm{RI}}$ as the ith eigenvalue of $\tilde{\mathbf{E}}_l^{\mathrm{RI}}$, we arrive at the following bound for RI

$$P\left(\mathbf{x}^{RI} \to \hat{\mathbf{x}}^{RI} | \{\mathbf{H}_k\}_{k=1}^{N_c}\right) \le \exp\left(-\frac{E_b}{N_o}d_1^2\sum_{i=1}^{LN_t}\sum_{j=1}^{N_r}\lambda_{i,1}^{\mathrm{RI}}\left|\hat{H}_{j,1}^i\right|^2\right) + \exp\left(-\frac{E_b}{N_o}d_2^2\sum_{i=1}^{LN_t}\sum_{j=1}^{N_r}\lambda_{i,2}^{\mathrm{RI}}\left|\hat{H}_{j,2}^i\right|^2\right).$$

Similarly as in the BI case, the PEP bound for RI is obtained as

$$P(\mathbf{x}^{RI} \to \hat{\mathbf{x}}^{RI}) \le \prod_{i=1}^{LN_t}\prod_{j=1}^{N_r}\frac{1}{1+d_1^2\frac{E_b}{N_o}\lambda_{i,1}^{\mathrm{RI}}} + \prod_{i=1}^{LN_t}\prod_{j=1}^{N_r}\frac{1}{1+d_2^2\frac{E_b}{N_o}\lambda_{i,2}^{\mathrm{RI}}}.$$

Let R denote the rank of the matrices $\tilde{\mathbf{E}}_l^{\mathrm{BI}}$ and $\tilde{\mathbf{E}}_l^{\mathrm{RI}}$. As R eigenvalues are nonzero. It follows that at high SNR, the PEP bounds for BI and RI are given by

$$P(\mathbf{x}^{BI} \to \hat{\mathbf{x}}^{BI}) \le \prod_{i=1}^{R}\left((d_1+d_2)^2\frac{E_b}{N_o}\lambda_{i,1}^{\mathrm{BI}}\right)^{-N_r} + \prod_{i=1}^{R}\left((d_1-d_2)^2\frac{E_b}{N_o}\lambda_{i,2}^{\mathrm{BI}}\right)^{-N_r} + \prod_{i=1}^{R}\left(d_1^2\frac{E_b}{N_o}\lambda_{i,3}^{\mathrm{BI}}\right)^{-N_r} \quad (7)$$

and

$$P(\mathbf{x}^{RI} \to \hat{\mathbf{x}}^{RI}) \le \prod_{i=1}^{R}\left(d_1^2\frac{E_b}{N_o}\lambda_{i,1}^{\mathrm{RI}}\right)^{-N_r} + \prod_{i=1}^{R}\left(d_2^2\frac{E_b}{N_o}\lambda_{i,2}^{\mathrm{RI}}\right)^{-N_r}. \quad (8)$$

For analytical conveniences, we assume that $\prod_{i=1}^{R}\left(\lambda_{i,l}^{\mathrm{BI}}\right)^{-N_r}$ and $\prod_{i=1}^{R}\left(\lambda_{i,l}^{\mathrm{RI}}\right)^{-N_r}$ are equal to $\lambda_{\mathrm{prod}}^{\mathrm{BI}}$ and $\lambda_{\mathrm{prod}}^{\mathrm{RI}}$ for all l, respectively. Simulation results confirm that this approximation turns out to be valid, as the elements of $\mathbf{S}_l^{\mathrm{BI}}$ and $\mathbf{S}_l^{\mathrm{RI}}$ are equally distributed for most-likely error events. As a result of the approximation, the above bounds (7) and (8) reduce to

$$P\left(\mathbf{x}^{BI} \to \hat{\mathbf{x}}^{BI}\right) \le \left((d_1+d_2)^{-2N_rR} + (d_1-d_2)^{-2N_rR} + d_1^{-2N_rR}\right)\left(\frac{E_b}{N_0}\right)^{-N_rR}\lambda_{\mathrm{prod}}^{\mathrm{BI}} \quad (9)$$

and

$$P\left(\mathbf{x}^{RI} \to \hat{\mathbf{x}}^{RI}\right) \le \left(d_1^{-2N_rR} + d_2^{-2N_rR}\right)\left(\frac{E_b}{N_0}\right)^{-N_rR}\lambda_{\mathrm{prod}}^{\mathrm{RI}}. \quad (10)$$

Now we analyze the diversity order of the proposed system. We see that the diversity order given by the above bound for BI and RI is determined by RN_r. We further examine the conditions on the rank R. Let us denote L_e as the instances $1 \le k \le N_c$ such that $\tilde{\mathbf{E}}_k^{BI} = \tilde{\mathbf{e}}_k^{BI}\left(\tilde{\mathbf{e}}_k^{BI}\right)^*$ or $\tilde{\mathbf{E}}_k^{RI} = \tilde{\mathbf{e}}_k^{RI}\left(\tilde{\mathbf{e}}_k^{RI}\right)^*$ is nonzero. Note that L_e is related to the effective length of the code [29]. Considering that $\tilde{\mathbf{E}}_k^{BI}$ and $\tilde{\mathbf{E}}_k^{RI}$ have rank one, we can show that the rank R of $\mathbf{\Lambda}^{\mathrm{BI}}{}_l$ or $\mathbf{\Lambda}^{\mathrm{RI}}{}_l$ is obtained by $\min(L_e, LN_t)$. Therefore, it can be seen here that the maximum achievable diversity order of this system for L tap equal power fading channels is $\min(L_e, LN_t)N_r$.

Next, we consider the coding gain in (9) and (10). For channels with large delay spreads, it should be noted that the slope change in BER curves due to additional antennas may not be as distinct as observed in flat fading channels [25]. In this case, optimizing the coding gain becomes more important in frequency selective channels. In general, $\lambda_{\mathrm{prod}}^{\mathrm{BI}}$ and $\lambda_{\mathrm{prod}}^{\mathrm{RI}}$ can be maximized by choosing an appropriate mapping and coding. One way of doing this is to increase the effective length of the code with an interleaver as suggested in [29]. Moreover, in order to improve the coding gain for BI and RI, we should optimize d_1 and d_2 in (9) and (10). As will be shown in the following simulation section, the error performance curves for BI and RI exhibit distinctive curve shapes in terms of d_2.

V. PERFORMANCE EVALUATION

In this section, we present simulation results to demonstrate the potential of our proposed UEP scheme and the two stage MLD over Rayleigh fading channels. A rate $\frac{1}{2}$ binary convolutional code with polynomials $(133, 171)$ in octal notation is used throughout the simulations. The OFDM modulation defined in the 802.11a standard with 64 point FFT is assumed. One OFDM symbol duration is set to 4 μs including the 0.8 μs guard interval. If not specified otherwise, a 5 tap multipath channel with an exponentially decaying delay profile is used in the simulations. Also two transmit antennas and two receive antennas are employed. We consider a system where a BER of 10^{-2} for RI is acceptable.

In Figs. 6 and 7, we present the performance comparison with uniform signal constellations between the proposed UEP and the conventional EEP in terms of BER. With the UEP scheme, a lower BER can be obtained for the BI bits at the expense of a higher BER on the RI bits. In the 16QAM case shown in Fig. 6, the proposed UEP scheme assumes $m_b = m_r = 2$. For both cases of MMSE and MLD, the BI performance of the proposed UEP demonstrates more than a 3 dB gain over the conventional EEP detector at a BER of 5×10^{-5}. Also the RI performance of the proposed UEP shows a 1 dB loss over the conventional EEP detector at a BER of 10^{-3}. The results of the 64QAM case in Fig. 7 are similar to those presented in the 16QAM case. In this case, the proposed UEP scheme can divide total information

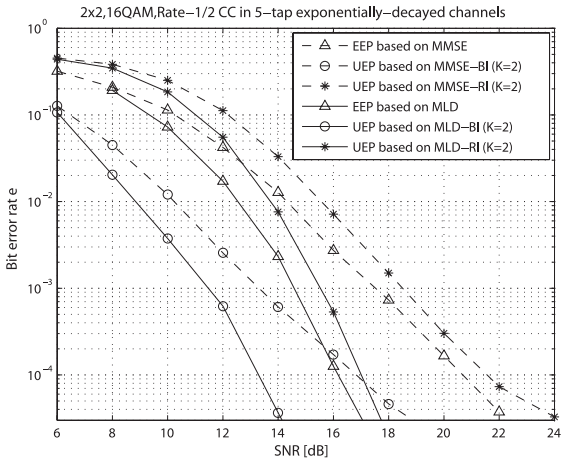

Fig. 6. Performance of the proposed UEP for 16QAM

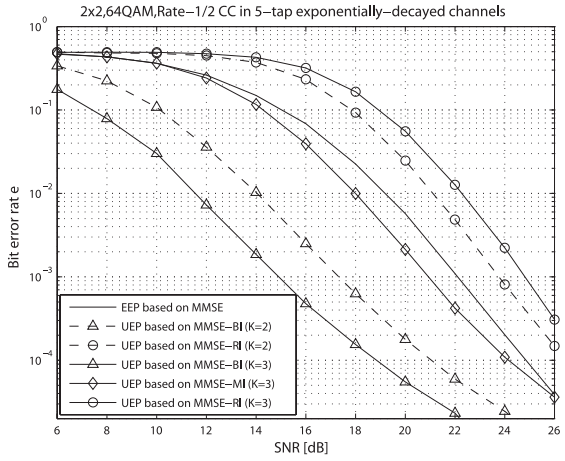

Fig. 7. Performance of the proposed UEP for 64QAM

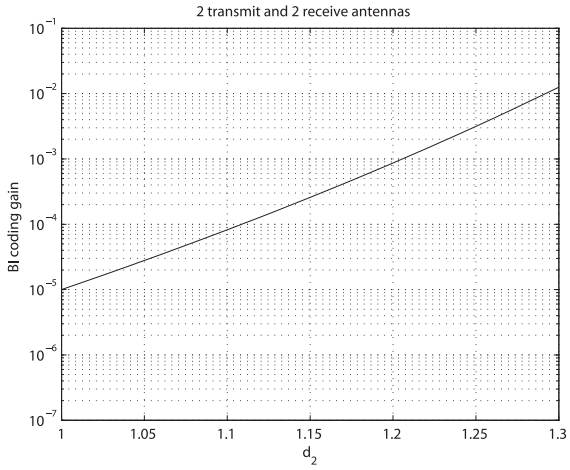

(a)

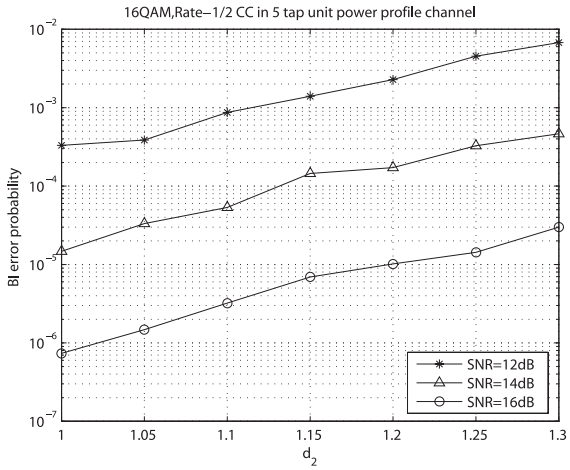

(b)

Fig. 8. Effect of d_2 on the BI error probability: (a) Theoretical performance, (b) simulated results.

into either two ($K = 2, m_b = m_r = 3$) or three groups ($K = 3, m_b = m_m = m_r = 2$), where m_m denotes the number of middle information (MI) bits. As can be seen in Fig. 7, the BI performance gain as well as the RI performance loss becomes greater when the information bits are divided by more than two groups. It should be noted that the RI performance is only 1 dB worse than the EEP case.

Now we will evaluate the PEP bounds of the BI and the RI bits derived in the previous section. Figs. 8 and 9 compare the bounds of the BI and RI error probabilities with actual simulations, respectively, for a 5 tap unit power channel profile with $d_1 = 2$. Figs. 8(a) and 9(a) plot the theoretical bound computed using the coding gain term in (9) and (10) for BI and RI. We can see that both plots change monotonically in terms of d_2 on the nonuniform signal constellation. Actually, simulation results presented in Figs. 8(b) and 9(b) show the similar pattern with the theoretical bound curves. These plots confirm that the performance bounds obtained in the previous section are quite accurate.

Also Fig. 10 illustrates the effect of d_2 on the BER of the overall information (OI) which is defined as all of the information bits. Here, the OI performance is obtained by averaging the BI and RI performance. We find that the OI performance is optimized with $1.2 < d_2 < 1.3$ for various SNR values.

Fig. 11 shows the BI, RI, and OI error performances of the UEP based on MLD with $d_2 = 1.25$ $\left(\lambda = \frac{1.25}{2}\right)$. In this plot, the OI performance gain of the UEP over the EEP case becomes 1.5 dB at a BER of 10^{-4}.

Fig. 12 presents simulation results with nonuniform signal constellations for the 16QAM case with different λ values. Here, the EEP assumes the uniform signal constellation. With increasing λ, the performance of the RI improves at the expense of the BI performance. Thus, λ can be optimized depending on system requirements such as the required BER of BI and RI. For $\lambda = \frac{1.25}{2}$, the OI performance of UEP based on MMSE is about 1 dB better than the EEP at a BER of 10^{-3}.

In Figs. 13 and 14, we show the performance of the proposed two stage MLD for the 16QAM and 64QAM cases, comparing with the conventional EEP receiver based on the MMSE and the full search MLD. For 16QAM, we assume $m_b = m_r = 2$. Both plots indicate that the performance gap between the proposed two stage MLD and the full MLD is very small. For the 64QAM

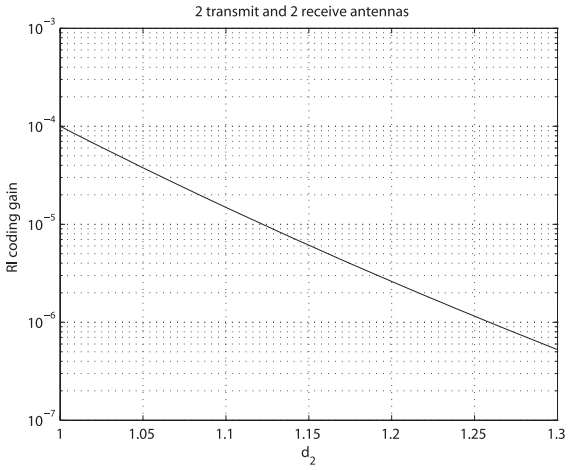

(a)

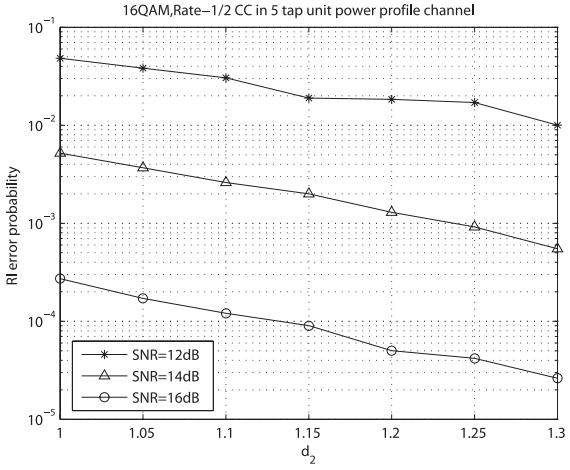

(b)

Fig. 9. Effect of d_2 on the RI error probability: (a) Theoretical performance, (b) simulated results.

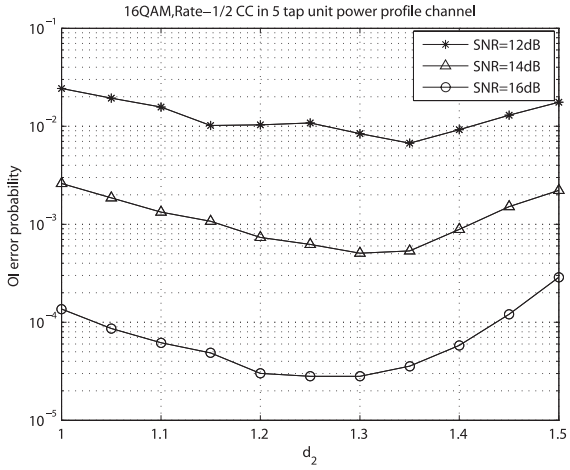

Fig. 10. Simulation results for OI

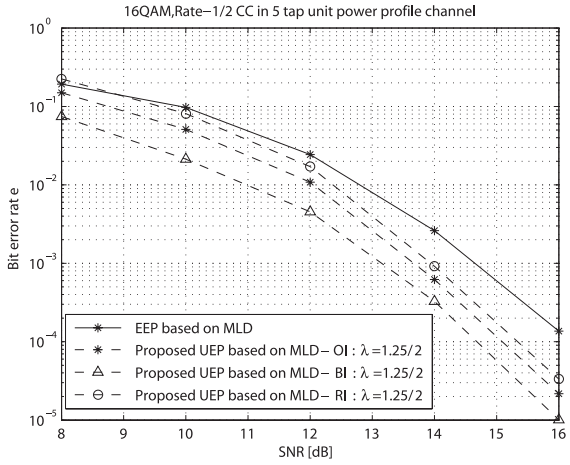

Fig. 11. Performance of the proposed UEP using the nonuniform signal constellation with MLD for 16QAM

case shown in Fig. 14, we change the number of RI bits. In this plot, we observe that as the number of BI and RI bits increases, the performance of the proposed scheme gets closer to that of the full search MLD algorithm. For the case of $m_b = 4$ and $m_r = 2$, the full MLD requires a search of 4096 candidates, while the proposed two stage MLD needs to search only 16 candidates. Thus, we conclude that the proposed two stage MLD method approaches the optimum MLD performance with much reduced complexity.

VI. CONCLUSION

In this paper, a new UEP scheme has been proposed and simulated for MIMO-OFDM systems with hierarchical signal constellations. Numerical results have demonstrated that a significant performance improvement can be obtained with the proposed detector compared with the conventional EEP detector. We have analyzed the pairwise error probability of the proposed UEP scheme for OFDM system with multiple antennas. Based on the analysis, we can evaluate the diversity and coding gain of the proposed UEP scheme with the nonuniform signal constellation. We can also maximize the coding gain by optimizing λ in the nonuniform signal constellation.

In addition, we have proposed a two stage MLD to reduce the complexity. A low complexity receiver is designed by decoupling a full MLD into two stages. Although this paper focuses on 16QAM or 64QAM with two transmit antennas, it is straightforward to generalize to arbitrary signal constellations with different antenna configurations.

REFERENCES

[1] R. H. Morelos-Zaragoza, L. Shu, and H. Imai, "Multilevel coded modulation for unequal error protection and multistage decoding–Part I: Symmetric constellations," *IEEE Trans. Commun.*, vol. 48, pp. 204–213, Feb. 2000.

[2] M. Isaka, M. P. C. Fossorier, R. H. Morelos-Zaragoza, S. Lin, and H. Imai, "Multilevel coded modulation for unequal error protection and multistage decoding–Part II: Asymmetric constellations," *IEEE Trans. Commun.*, vol. 48, pp. 774–786, May 2000.

[3] D. Boudreau, R. Lyon, G. Gallinaro, and R. De Gaudenzi, "A simulation of audio and video telephony services in a satellite UMTS environment," in *Proc. IMSC*, June 1999, pp. 220–225.

[4] J. Hagenauer, "Rate-compatible punctured convolutional codes (RCPC

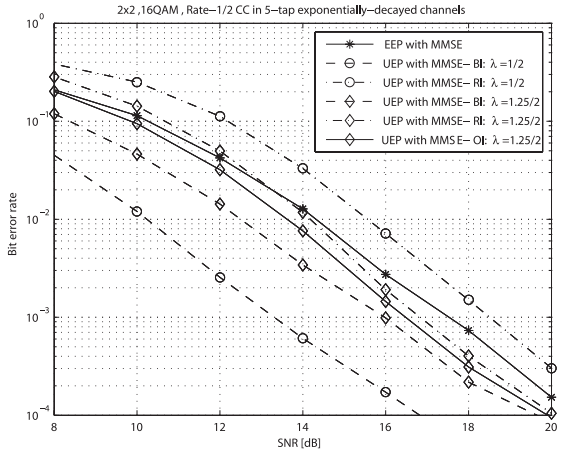

Fig. 12. Performance of the proposed UEP using the nonuniform signal constellation with MMSE for 16QAM

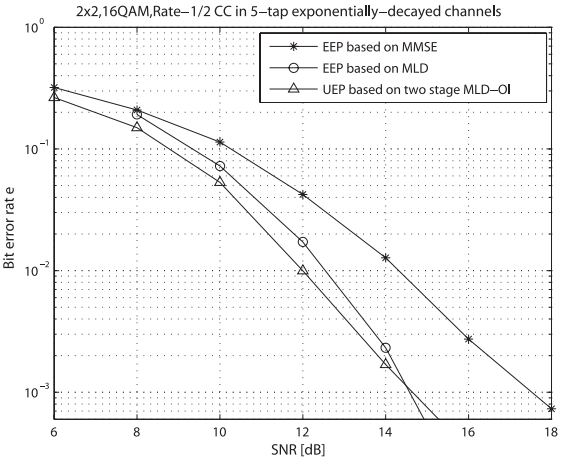

Fig. 13. Performance of the proposed two stage MLD for 16QAM

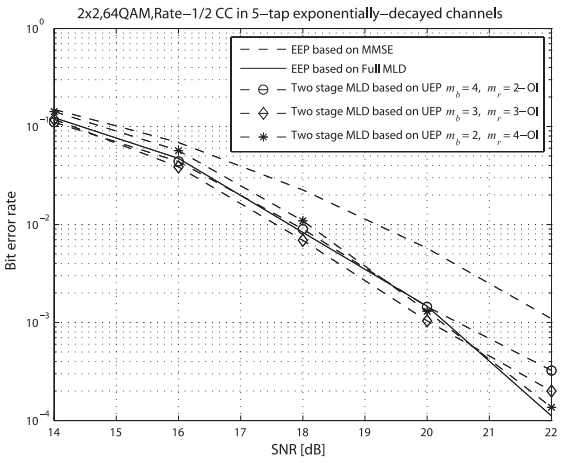

Fig. 14. Performance of the proposed two stage MLD for 64QAM

codes) and their applications," *IEEE Trans. Commun.*, vol. 36, pp. 389–400, Apr. 1998.

[5] R. V. Cox, J. Hagenauer, N. Seshadri, and C.-E. W. Sundberg, "Subband speech coding and matched convolutional channel coding for mobile radio channels," *IEEE Trans. Acoust., Speech, Signal Process.*, vol. 39, pp. 1717–1731, Aug. 1991.

[6] H. Imai and S. Hirakawa, "A new multilevel coding method using error correcting codes," *IEEE Trans. Inf. Theory*, vol. 23, pp. 371–377, May 1977.

[7] N. Seshadri and C.-E. W. Sundberg, "Multilevel trellis coded modulations for the Rayleigh fading channel,"*IEEE Trans. Commun.*, vol. 41, pp. 1300–1310, Sept. 1993.

[8] P. K. Vitthaladevuni and M.-S. Alouini, "A closed-form expression for the exact BER of generalized PAM and QAM constellations," *IEEE Trans. Commun.*, pp. 698–700, May 2004.

[9] G. J. Foschini, "Layered space-time architecture for wireless communication in a fading environment when using multi-element antennas," *Bell Labs. Tech. J.*, vol. 1, pp. 41–59, Autumn 1996.

[10] I. E. Telatar, "Capacity of multi-antenna Gaussian channels," *Eur. Trans. Telecom.*, vol. 10, pp. 585–595, Nov. 1999.

[11] S. L. Ariyavisitakul, J. H. Winters, and I. Lee, "Optimum space-time processors with dispersive interference: Unified analysis and required filter span," *IEEE Trans. Commun.*, vol. 48, pp. 1347–1359, Aug. 2000.

[12] L. J. Cimini, "Analysis and simulation of a digital mobile channel using orthogonal frequency division multiplexing," *IEEE Trans. Commun.*, vol. 33, pp. 665–675, July 1985.

[13] J. A. Bingham, "Multicarrier modulation for data transmission: An idea whose time has come," *IEEE Commun. Mag.*, pp. 5–14, May 1990.

[14] H. Sari, G. Karam, and I. Jeanclaude, "Transmission techniques for digital terrestrial TV broadcasting," *IEEE Commun. Mag.*, vol. 33, pp. 100–109, Feb. 1995.

[15] R. van Nee, G. Awater, M. Morikura, H. Takanashi, M. Webster, and K. W. Halford, "New high-rate wireless LAN standards," *IEEE Commun. Mag.*, vol. 37, pp. 82–88, Dec. 1999.

[16] J. Li, K. B. Letaief, and Z. Cao, "A reduced-complexity maximum-likelihood method for multiuser detection," *IEEE Trans. Commun.*, vol. 52, pp. 289–295, Feb. 2004.

[17] K. B. Letaief, E. Choi, J.-Y. Ahn, and R. Chen, "Joint maximum likelihood detection and interference cancellation for MIMO/OFDM systems," in *Proc. IEEE VTC*, Oct. 2003, pp. 612–616.

[18] H. Artes, D. Seethaler, and F. Hlawatsch, "Efficient detection algorithms for MIMO Channels: A geometrical approach to approximate ML detection," *IEEE Trans. Signal Process.*, vol. 51, pp. 2808–2820, Nov. 2003.

[19] X. Liand, H. C. Huang, A. Lozano, and G. J. Foschini, "Reduced-complexity detection algorithms for systems using multi-element arrays," in *Proc. IEEE GLOBECOM*, Dec. 2000, pp. 1072–1076.

[20] I. Lee and C.-E. W. Sundberg, "Reduced complexity receiver structures for space-time bit-interleaved coded modulation systems," *IEEE Trans. Commun.*, vol. 55, pp. 142–150, Jan. 2007.

[21] P. K. Vitthaladevuni and M.-S. Alouini, "BER computation of 4/M-QAM hierarchical constellations," *IEEE Trans. Broadcasting*, vol. 47, pp. 228–239, Sept. 2001.

[22] K. Ramchandran, A. Ortega, K. M. Uz, and M. Vetterli, "Multiresolution broadcast for digital HDTV using joint source/channel coding," *IEEE J. Sel. Areas Commun.*, vol. 11, pp. 6–23, Jan. 1993.

[23] F. Tosato and P. Bisaglia, "Simplified soft-output demapper for binary interleaved COFDM with application to HIPERLAN/2," in *Proc. IEEE ICC*, Sept. 2002, pp. 664–668.

[24] X. Li, H. Huang, G. J. Foschini, and R. A. Valenzuela, "Effects of iterative detection and decoding on the performance of BLAST," in *Proc. IEEE GLOBECOM*, Dec. 2000, pp. 1061–1066.

[25] I. Lee, A. M. Chan, and C.-E. W. Sundberg, "Space-time bit-interleaved coded modulation for OFDM systems," *IEEE Trans. Signal Process.*, vol. 52, pp. 820–825, Mar. 2004.

[26] M. Sajadieh, F. R. Kschischang, and A. Leon-Garcia, "Modulation-assisted unequal error protection over the fading channel," *IEEE Trans. Veh. Technol.*, pp. 900–908, Aug. 1998.

[27] P. K. Vitthaladevuni and M.-S. Alouini, "A Recursive algorithm for the exact BER computation of generalized hierarchical QAM constellations," *IEEE Trans. Inf. Theory*, vol. 49, pp. 297–307, Jan. 2003.

[28] T. S. Rappaport, *Wireless Communication, Priciples and Practice*. New Jersey: Prentice-Hall, 1996.

[29] V. Tarokh, N. Seshadri, and A. R. Calderbank, "Space-time codes for high data rate wireless communication: Performance criterion and code construction," *IEEE Trans. Inf. Theory*, vol. 44, pp. 744–765, Mar. 1998.

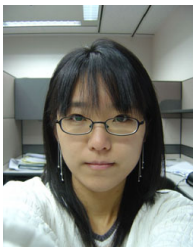

Yujin Noh was born in Seoul, Korea, on June 1, 1980. She received the B.Sc. degree in Electrical, Electronics and Radio Engineering and the M.Sc. in Radio Sciences and Engineering from the Korea University, Korea, in 2004 and 2006, respectively. From January 2006 to February 2007, she worked for Intel Korea R&D center, Korea. Presently, she is a researcher in LG Electronic.

Heunchul Lee received the B.S. degree in Electrical Engineering in 2003 and the M.S. degree in Radio Communications Engineering in 2005, both from Korea University, Seoul, Korea, where he is currently working toward the Ph.D. degree in the School of Electrical Engineering. During the winter of 2006, he worked as an intern at Beceem Communications, Santa Clara, CA, USA. His research interests include space-time coding, signal processing, and coding for wireless communications, with current emphasis on signal processing techniques for MIMO-OFDM systems. He received the Best Paper Award at the 12th Asia-Pacific conference on Communications, and the IEEE Seoul Section Student Paper Contest award, both in 2006.

Wonjun Lee is an associate professor in the Department of Computer Science and Engineering at Korea University, Seoul, Korea. He received the B.S. and M.S. degrees in computer engineering from Seoul National University, Seoul, Korea in 1989 and 1991, respectively. He also received the M.S. in computer science from the University of Maryland, College Park, USA in 1996 and the Ph.D. in computer science and engineering from the University of Minnesota, Minneapolis, USA, in 1999. His research interests include mobile wireless communication protocols, RFID protocols, wireless mesh network protocols, and Internet architecture technology. He has authored or co-authored over 80 papers in refereed international journals and conferences. He is a Senior Member of IEEE.

Inkyu Lee was born in Seoul, Korea in 1967. He received the B.S. degree (Hon.) in control and instrumentation engineering from Seoul National University, Seoul, Korea in 1990, and the M.S. and Ph.D. degrees in electrical engineering from Stanford University, Stanford, CA in 1992 and 1995, respectively. From 1991 to 1995, he was a Research Assistant at the Information Systems Laboratory, Stanford University. From 1995 to 2001, he was a Member of Technical Staff at Bell Laboratories, Lucent Technologies, where he studied the high-speed wireless system design. He later worked for Agere Systems (formerly, Microelectronics Group of Lucent Technologies), Murray Hill, NJ as a Distinguished Member of Technical Staff from 2001 to 2002. In September 2002, he joined the faculty of Korea University, Seoul, Korea, where he is currently an Associate Professor in the School of Electrical Engineering. He has published over 30 journal papers in IEEE, and has 20 U.S. patents granted or pending. His research interests include digital communications, signal processing, and coding techniques applied to wireless systems. He currently serves as an Associate Editor for the IEEE TRANSACTIONS ON COMMUNICATIONS in the area of Wireless Communication Theory and has also been a Chief Editor for the IEEE JOURNAL ON SELECTED AREAS IN COMMUNICATIONS (Special Issue on 4G Wireless Systems) in 2006. Dr. Lee received the IT Young Engineer Award as the IEEE/IEEK joint award in 2006. Also in 2006, he received the APCC '06 best paper award.